Journal of Materials Chemistry A

Accepted Manuscript

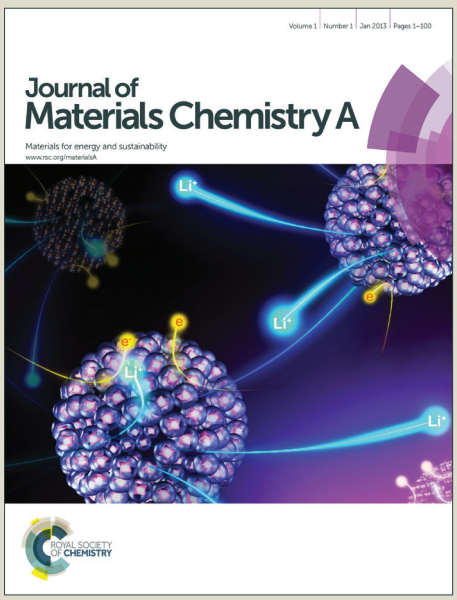

ROYAL SOCIETY OF CHEMISTRY

www.rsc.org/materialsA

Journal of Materials Chemistry A RSCPublishing

PAPER

Multifunctional Graphene Sheet-Nanoribbon Hybrid Aerogels

Cite this: DOI: 10.1039/x0xx00000x

Chunhui Wang,[1] Xiaodong He,[1] Yuanyuan Shang,[1,2] Qingyu Peng,[1] Yuyang Qin,[1] Enzheng Shi,[2] Yanbing Yang,[2] Shiting Wu,[2] Wenjing Xu,[2] Shanyi Du,[1] Anyuan Cao,[2*] Yibin Li[1*]

Received 00th January 2012,
Accepted 00th January 2012

DOI: 10.1039/x0xx00000x

www.rsc.org/

Graphene sheets and nanoribbons are graphene-based nanostructures with different dimensions. Here, we show that these two materials can be combined to form highly porous, ultra-low density, compressible yet elastic aerogels, which can be used as efficient adsorbents and supercapacitor electrodes. The pore walls consist of stacked graphene sheets embedded with uniformly distributed thick nanoribbons unzipped from multi-walled carbon nanotubes as effective reinforcing skeletons. Owing to the large pore-size, robust and stable structure, and the nanoribbon-adhered pore walls, these hybrid aerogels show very large adsorption capacity for a series of organic solvents and oils (100 to 350 times of aerogel weight), and a specific capacitance of 256 F/g tested in a three-electrode electrochemical configuration, which is further improved to 537 F/g by depositing controlled loading pseudo-polymers into the aerogels. Our multifunctional graphene sheet-nanoribbon hybrid aerogels may find potential applications in many fields such as environmental cleanup, and flexible electrodes for energy storage systems such as supercapacitors and batteries.

Introduction

Graphene is a typical two-dimensional (2D) carbon nanostructure with fascinating mechanical and electrical properties.[1,2] Liquid exfoliation is a widely studied method to produce graphene oxide (GO) sheets from graphite powders in large scale.[3] The as-produced uniform suspensions of GO sheets can be self-assembled into three-dimensional (3D) porous networks (hydrogels and aerogels) by simple methods such as thermal aggregation (cross-linking) or casting.[4,5] Graphene aerogels in the form of monolithic blocks or continuous fibers exhibit light-weight, high porosity, excellent mechanical strength and flexibility, and have attracted tremendous interest in the past years.[6-10] Extensive study in this area has demonstrated potential applications as adsorbents, sensors, electrodes, electrocatalysts of graphene and functionalized graphene aerogels.[11-14] One of the emerging research directions is to fabricate hybrid graphene-based materials, in which other nanostructures or functional materials are introduced into the graphene framework to not only reinforce the network structure, but also enable new applications and improve performance.[15] For example, multi-walled carbon nanotubes (CNTs) were grafted onto the graphene walls forming a CNT-coated graphene structure and the graphene-CNT hybrid aerogels became elastic under compression.[16] Amorphous porous carbon was grafted into graphene aerogels to increase surface area.[17] Aligned CNTs or mesoporous carbons were also synthesized within the graphene foam supported on a nickel framework to fabricate high specific surface area and conductive supercapacitor electodes.[18,19] In addition, hybrid aerogels by coating graphene with multi-walled nanotubes or partially unzipping a CNT sponge have been reported recently.[20,21]

To date, most of hybrid aerogels are based on the graphene-CNT system. In addition to CNTs, graphene nanoribbons (GNRs) are thin strips of graphene made by unzipping CNTs along the tube axis.[22] They have a similar aspect ratio to CNTs yet also a planar structure like graphene sheets, with unique chemical and physical properties.[23,24] GNRs also found many applications as fillers in nanocomposites, and as charge transport paths in solar cell and battery electrodes.[25-27] Despite of some methods such as patterned growth or etching,[28,29] the only scalable approach to yield GNRs is to unzip CNTs (usually more effective for multi-walled nanotubes) by chemical oxidation.[30,31] These GNRs have extensive defects

[1]*Center for Composite Materials and Structures, Harbin Institute of Technology, Harbin 150080, P. R. China*
[2]*Department of Materials Science and Engineering, College of Engineering, Peking University, Beijing 100871, P. R. China*
**Corresponding authors. Email: liyibin@hit.edu.cn, anyuan@pku.edu.cn*

and non-uniform widths (and thickness), and are more suitable for mechanical (versus electrical) applications.

Here, we introduce GNRs into GO sheets to make highly porous aerogels with a unique GO-GNR hybrid pore wall structure. We use relatively thick GNRs by chemically unzipping multi-walled CNTs to reinforce the graphene aerogels, leading to enlarged pore sizes and significantly enhanced elasticity after compression. Our GO-GNR aerogels show high adsorption capacity (100 to 350 times of own weight) to organic solvents and oils, and can be used repeatedly. The open porous structure also allows direct deposition of pseudo-materials to make high performance supercapacitor electrodes, with a specific capacitance of 256 F/g for pristine aerogels and 537 F/g for pseudo-polymer loaded aerogels.

Experimental

Synthesis of Graphene Oxide and Graphene Nanoribbons

Graphene oxide was synthesized from graphite according to a modified Hummers' method.[32] Typically, natural graphite powders were annealed at 1000 °C for 2 h to get expanded graphite, and then the as-prepared black powders (7.7 g) were put into an solution of concentrated H_2SO_4 (900 mL), H_3PO_4 (100 mL), and $KMnO_4$ (50 g). After being stirred with a magnetic bar for 5 h at 50 °C, the mixture was poured into an ice bath containing a small amount of hydrogen peroxide (H_2O_2, 30%). The golden solution was filtered and the resulting slurry was washed with 10% HCl and water by centrifugation at 9500 rpm (in order to remove the SO_4^{2-} and unoxidized graphite impurities), until the pH of the supernatant was adjusted to 5. The brown residues were carefully collected and then diluted to a desired concentration. Graphene nanoribbons were synthesized by lengthwise cutting of multi-walled CNTs, as reported by James Tour and co-workers.[22] 1 g multi-walled CNTs were added to 180 mL concentrated H_2SO_4 and stirred at room temperature for 2 h (to fully exfoliate the nanotube). H_3PO_4 (85%, 20 mL) was then added to the dispersion, and the mixture was stirred for another 15 min followed by addition of 8 g $KMnO_4$ (slowly added within 1 h). The reaction mixture was heated to 65 °C for 2 h until the color of the solution became reddish brown, and then cooled to room temperature. Subsequently, the reaction mixture was poured into 500 mL ice containing of 10 mL H_2O_2 (30%), and placed overnight. The supernatant was filtered and the products were washed with 10% HCl (2 × 200 mL), ethanol (2 × 50 mL), and water (2 × 100 mL) by centrifugation.

Preparation of GO-GNR Aerogels and GO-GNR@Polypyrrole

GO-GNR aerogels synthesis was performed using a freeze-drying method. Typically, GO and GNR aqueous dispersions were mixed together and the ratio of GO to GNR by weight was kept at 1:1, the mixture was stirred for 1 h followed by pouring into a mold. Subsequently, the solution was frozen for 2 h followed by freeze-drying for 24 h. The as-prepared foam was chemically reduced by hydrazine vapor at 90 °C for 24 h. Aerogels with different shape can be obtained according to this method by adjusting the mold. GO-GNR aerogels with a range of densities (from 1.0 to 13 mg cm^{-3}) were prepared under the same conditions except using different concentrations of GO and GNR mixture. For the preparation of polypyrrole (PPy)-coated composite aerogels, GO-GNR aerogels were immersed in 0.3 M $NaClO_4$ aqueous solution containing 5 % (V: V) pyrrole. The aerogels were directly used as the working electrode under a potential of 0.8 V. The electro-deposition process of PPy was performed in a three-electrode electrochemical workstation (CHI660D instruments, shanghai, China) for 50 s (resulting in a PPy loading of 16.4 wt%), 200 s (37.2 wt%), 300 s (49.1 wt%). A Pt wire and Ag/AgCl were used as the counter and reference electrodes, respectively. After the electropolymerization process, the as-prepared aerogels were rinsed with distilled water and then subjected to freeze-drying.

Adsorption Experiment

The initial weight of a monolithic aerogel was recorded as M_0. After immersed in the oil, the aerogel became saturated by oil adsorption. Then the aeogel was taken out for weighing again with the weight recorded as M_t after adsorption. The oil adsorption capacity (Q) of the aerogel was calculated and estimated using the following equation (1):

$$Q\ (g/g) = (M_t - M_0)/M_0 \quad (1)$$

Electrochemical Characterization

All electrochemical measurements were carried out in a three-electrode system using an electrochemical workstation (CHI660D, Chenhua Instruments, China) with 2 M KCl solution as the electrolyte. The as prepared porous materials were directly used as the electrode. Typically, a thin slice of the aerogel was split from the monoliths and clamped by two polymeric blocks. Platinum wires twisted around the polymeric clamps and connected to the aerogel electrode were used as current collectors while Pt wire and Ag/AgCl as the counter and reference electrodes. The electrochemical performances of the prepared electrodes were characterized by cyclic voltammetry, galvanostatic charge-discharge tests. The specific capacitance was obtained from the CV curves according to the following equation (2):

$$C_{cell} = \int \frac{I}{m} dV / v\Delta V \quad (2)$$

where I is the response current (A), m is the total mass of aerogel electrodes (g), ΔV is the potential range (V), v is the potential scan rate (mV/s).

Results and Discussions

Our hybrid GO-GNR aerogels were fabricated through the following process, as illustrated in Figure 1. GO sheets were obtained by liquid exfoliation of expanded graphite by the

modified Hummers' method.[32] GNRs were prepared through solution-based chemical unzipping of multi-walled CNTs (diameters of 30-80 nm),[22] resulting in nanoribbons with thicknesses of 0.5-4.5 nm and widths of 50-200 nm. Separated suspensions of GO sheets and GNRs with controlled concentrations were mixed together by magnetic stirring (The ratio of GO to GNRs by weight was kept consistent at 1:1). The resulting homogeneous mixture in a glass container was subjected to freezing and freeze-drying to form a porous aerogel (see Experimental for details). When necessary, chemical reduction by hydrazine was performed on the aerogel to render it elastic. During the self-assembly (aggregation) of GO sheets and the formation of a 3D network, GNRs mixed among the GO sheets were also included into the pore walls, forming the hybrid aerogel (Fig. 1a).

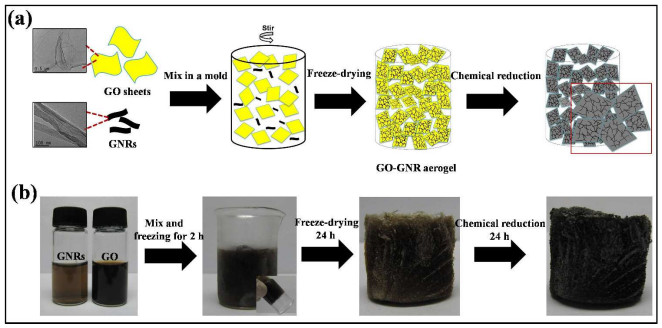

Figure 1. Illustration of the fabrication process of the GO-GNR aerogel. a) GO sheets and GNRs were mixed together by stirring, the mixture was subjected to freezing and freeze-drying, followed by chemical reduction if necessary. b) Photos of GNRs, GO suspensions and GO-GNR aerogel before and after reduction.

By adjusting the initial concentrations of GO and GNR suspensions (1.2 to 13.6 mg mL^{-1}), hybrid aerogels with densities ranging from 1.0 to 13 mg cm^{-3} (after chemically reduced) were fabricated correspondingly. The lowest density aerogels still allow careful manipulation without collapse. A cylindrical aerogel with a volume of 6.0 cm^{-3} and density of 2.2 mg cm^{-3} has a weight of 13.2 mg, which is lighter compared to a red bean with diameter of 0.5 cm (Fig. 2a). In addition to cylinders, heart-shaped monolith and large size discs (23.5 cm in diameter and 1.5 cm in thickness) were also produced, indicating that our process is scalable (Fig. 2b, 2c). The porous structure which appears on the aerogel surface can even be distinguished by naked eyes.

We have characterized the microstructure of these hybrid aerogels by scanning electron microscopy (SEM). The as-prepared aerogels are constructed by interconnected graphene sheets via partial overlapping by π-π interactions in a 3D configuration, resulting in a highly porous network (Fig. 2d). To further characterize the physical properties of GO-GNR aerogels, N_2 adsorption/desorption analysis was performed and the results indicating the porous structure of our aerogels, the pores of our aerogels are larger than 2.5 nm and have a wide size distribution from 2.5 nm to 35 nm. (Supporting Information, Fig. S1). This porous structure looks similar to previously reported graphene aerogels, however, we find that some micro-pore sizes are more than 100 μm (Fig. 2e), which are larger than conventional graphene counterparts (usually with pore size of 5-70 μm).[6-8] The porous structure lead to very low density of our aerogels, and also enable direct polymer deposition as well as liquid infiltration as described later.

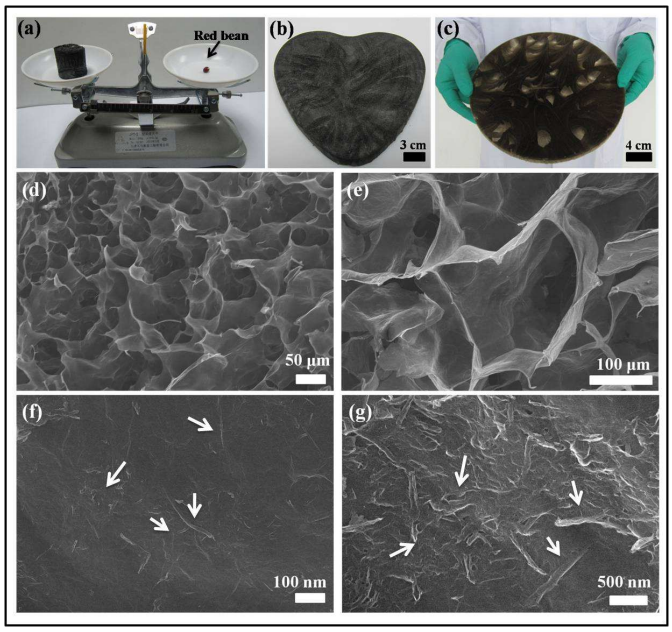

Figure 2. a) The weight of a cylindrical aerogel (13.2 mg, ρ = 2.2 mg cm^{-3}) is lighter than a red bean (0.1 g, with diameter of 0.5 cm). b) A heart shaped aerogel (ρ = 5.8 mg cm^{-3}). c) A~650 cm^3 GO-GNR aerogel cylinder with a diameter of 23.5 cm and 1.5 cm in thickness (ρ = 3.5 mg cm^{-3}). d) Porous structure of the GO-GNR aerogel. e) Morphology of a typical pore of the GO-GNR aerogel. The diameter of the pore is larger than 100 μm. f) Morphology of GNRs coated on graphene sheets (white arrows show GNRs attached or embedded within the graphene wall). g) High-magnification SEM images of the as-prepared aerogel, showing GNRs coated graphene sheet pore-walls (white arrows point to the GNRs attached to the GO sheets).

Close view on the pore walls reveals many nanoribbon features uniformly attached or embedded within the graphene wall (Fig. 2f, 2g). These GNRs maintain the original flat and ribbon-like morphology (with lengths of tens to hundreds of nm), and most of them are distributed individually without forming aggregations, indicating that they have been mixed with GO sheets homogeneously in the suspension for freeze-drying. The presence of GNRs can be clearly distinguished, as they also make the pore walls rough. Given the flat morphology of both GO sheets and GNRs as well as their π-π interaction, here we obtain a coherent hybrid porous structure consisting of large-size 2D sheets and smaller size nanoribbons, which is different from previous GO-CNT hybrid aerogels.[16] The strong adhesion of GNRs to the GO sheets has also been confirmed by transmission electron microscopy (TEM) images where the GO-GNR hybrid structure is maintained after dispersing the aerogel by vigorous sonication (Fig. S2).

To analyze the evolution of oxygen-containing groups during the preparation procession, FT-IR was adopted (Fig. S2). The

GO-GNR hybrid aerogels before reduction has two characteristic peaks: C=O stretching vibrations from carbonyl and carboxyl groups (approximately 1720 cm^{-1}), C-O stretching vibration from epoxyl (approximately 1220 cm^{-1}). These mainly attribute to the oxidation groups of GONR and GO. After being reduced by hydrazine, the oxidation peaks vanished, leaving only C=C stretching peak (approximately 1620 cm^{-1}), reflecting that the oxygen-containing groups is removed. X-ray diffraction (XRD) spectra provide further evidence for the reduction (Fig. S2), the typical diffraction peak for graphene oxide at around 11° has disappeared, leaving a broad diffraction peak at 2θ=24.8° corresponding to the graphitic structure in the reduced GO-GNR aerogels.[9] Also, X-ray photoelectron spectroscopy (XPS) analysis were conducted to investigate the evolution of oxygen-containing species (Fig. S3). The C_{1s} spectrum of GO-GNR aerogels before reduction can be deconvoluted in four peaks at 284.5, 286.7, 287.8 and 289 eV, corresponding to C-C and C=C of aromatic rings, C-O of epoxyl, C=O and O-C=O of carboxyl groups. After being chemically reduced, the peak intensity of C=C rises dramatically while C-O, C=O and O-C=O decrease sharply indicating the removal of oxygen-containing groups. After the reduction, the color of the aerogels turns from brown to black with about 25 wt% loss while the 3D network is maintained indicative of strong interconnection between GO-GNR building blocks (Fig. 1b).

Our hybrid aerogels exhibit excellent flexibility and elasticity after the chemical reduction. The aerogels can recover to original morphology after being compressed to 60% and

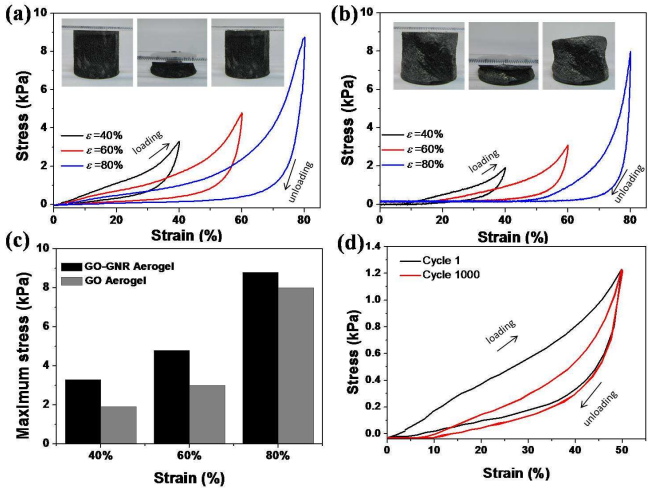

Figure 3. a, b) The stress-strain curves of GO-GNR aerogel (8 cm^{-3} in volume, containing 27.2 mg GO and 27.2 mg GNR, with density of 6.8 mg cm^{-3} before reduction) and GO aerogel (8 cm^{-3} in volume, containing 27.2 mg GO without adding GNRs, with a density of 3.4 mg cm^{-3} before reduction) at different maximum strain of 40%, 60% and 80%, respectively. Insets are digital images showing compressibility of GO-GNR aerogel and GO aerogel, respectively. All the samples were chemically reduced before test. c) The maximum stresses of sample (a) and (b) at maximum strain of 40%, 60% and 80%. f) The stress-strain curves of sample (a) at the maximum strain of 50% for 1000 cycles.

removing the external load (inset of Fig. 3a). Compressive stress-strain (σ-ε) curves with set strains up to 40%, 60%, and 80% show three distinct stages (Fig. 3a), including a linear-elastic regime during which the stress increases linearly at ε < 20%, a plateau region at 20% < ε < 70% and a steep slope region at ε > 70% with rapidly stress rising because of the densification of aerogels. Even at the strain of ε = 80%, our GO-GNR aerogels can recover elastically with a small residual strain (<3%). We also fabricated neat graphene aerogels (GO aerogels) control samples consisting of only GO sheets without adding GNRs. After reduction, the GO aerogels recover only partially with a plastic deformation of 15% and 50% at the strain of 60% and 80%, respectively, upon removal of the external load (Fig. 3b). This result indicates that the introduction of GNRs could enhance the elasticity, and we attribute the enhanced mechanical properties to the GNR-coated graphene structure which combine the advantages of GNRs with graphene sheets. The flat GNRs adhered strongly with GO sheets due to the π-π interaction and the reinforcement makes these GO-GNR composite sheets are more robust than neat graphene sheets (Fig. 3c). Cyclic tests were also conducted (Fig. 3d), the hysteresis loop for the 1000th cycle curve shrinks compared to the first one, but the maximum stress remains unchanged, indicating that our hybrid aerogels can retain the compressive strength after repeated compression for 1000 cycles at the strain of 50%.

Our aerogels having large-size pores and robust porous structure are suitable candidate for adsorption. To this end, we investigated their adsorption capacity for oils and organic liquids. When an aerogel was placed on a floating diesel oil membrane on water, the GO-GNR aerogel selectively adsorbed the diesel oil and was remain floated on water (Fig. 4a).

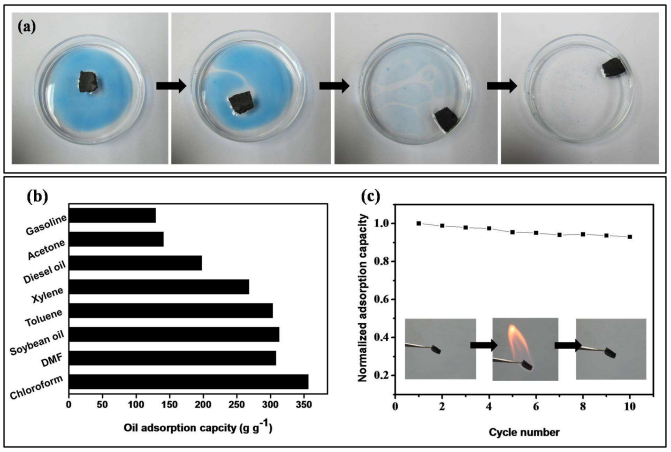

Figure 4. a) GO-GNR aerogel adsorbing diesel oil dyed with Oracet blue B. b) Adsorption capacity of GO-GNR aerogel for various organic liquids. c) Recyclability of the GO-GNR aerogel tested with hexane. The adsorption capacity after 10 cycles is normalized by the initial weight gain.

The high porosity and robust GO-GNR skeleton of our aerogels provide an ideal platform for high-efficiency adsorption of oil and it takes a few seconds to reach saturation. To further investigate the adsorption capacities of our aerogels, several other organic solvents were tested (Fig. 4b). The adsorption

capacity (Q) values for GO-GNR aerogels for all the organic solvents tested were over 100 g g^{-1} and among those the highest capacity was 350 g g^{-1} for chloroform. This is a quite high value compared with other graphene-based aerogels reported (22-160 g g^{-1}).[11,33,34] Additionally, we tested the recyclability of our aerogels with hexane by burning the solvents adsorbed. After ten cycles, GO-GNR aerogels retain 90% of the absorption capacity and maintain the 3D structure without structural collapse (Fig. 4c).

The rich open-pore structure of our aerogels is favorable for electrolyte infiltration, making them an effective electrode material for double-layer supercapacitors. To investigate the electrochemical property, we tested the chemically reduced GO-GNR aerogels as electrodes for supercapacitors in a three-electrode system. Fig. 5a shows the cyclic voltammograms (CVs) of the GO-GNR electrode at different scan rates from 2 to 100 mV s^{-1}. The CV curves exhibit typical quasi-rectangular shape, especially at 2 mV s^{-1}, indicating good charge transportation at the electrode interface according to the mechanism of the double-layer capacitor. The highest specific capacitance reaches 256 F g^{-1} at a scan rate of 2 mV s^{-1} (Fig. 5b), which is comparable with the best performance of supercapacitors made by other graphene aerogels in recent reports (Summarized in Table S1).[S1-S5]

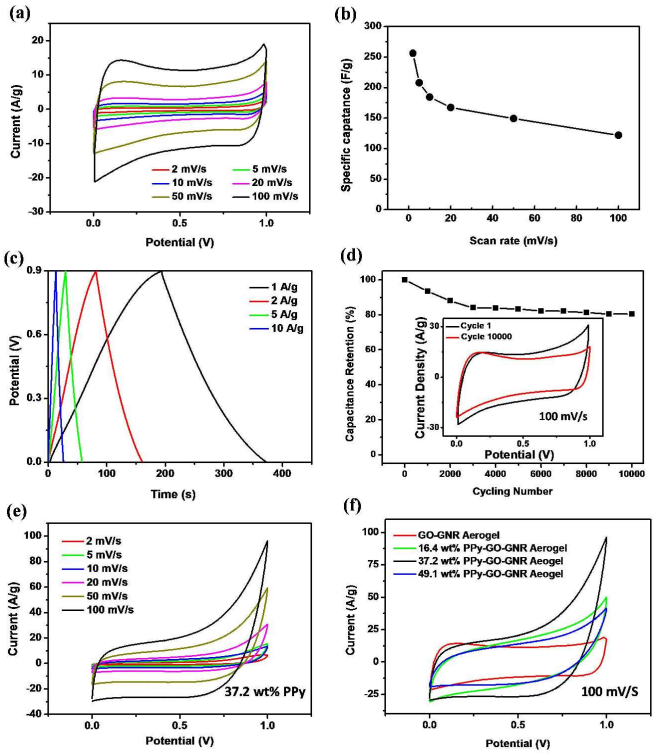

Figure 5. a) CVs of a GO-GNR electrode in 2 M KCl aqueous solution. b) Calculated specific capacitances of the GO-GNR electrode. c) The galvanostatic charge-discharge curves at a current density of 1, 2, 5, and 10 A/g. d) Cycling tests showing a capacitance retention of > 80% after 10000 charging and discharging cycles at 100 mV/s. Inset shows the CV curves for cycle 1 and cycle 10000, repectively. e) CVs of a PPy-coated GO-GNR electrode in 2 M KCl aqueous solution. f) CVs of different PPy loaded GO-GNR aerogels and pristine aerogels at a scan rate of 100 mV/s in 2 M KCl.

With increasing scan rate, the current response increased accordingly and the specific capacitance of our electrode maintains 47.5% specific capacitances with a value of 122 F g^{-1} as the scan rate increased to 100 mV s^{-1}. The galvanostatic charge-discharge (GCD) curves of our electrode at four different current densities (1, 2, 5, 10 A/g) are shown in Fig. 5c. The linear and symmetric triangular shape of the GCD curve is also the feature of double layer capacitance which demonstrates that our electrodes possess excellent electrochemical reversibility and charge-discharge properties. The specific capacitance calculated from GCD curve is 200 F g^{-1} at a current density of 1 A g^{-1}. We have tested the CV cycling stability of our electrode for 10000 cycles at a scan rate of 100 mV s^{-1} (Fig. 5d). It is found that the capacitance retention of our electrode maintains 80.4% after 10000 charging and discharging cycles, suggesting a good cycling stability for our material. Also, we fabricated a GO-GNR@Polypyrrole (PPy) composite electrode by introducing conductive polymer PPy onto GO-GNR sheets. Owing to the large-size pores, our PPy-coated aerogels can be fabricated easily by directly electrochemical deposition in pyrrole solution (see Experimental for details). The robust GO-GNR sheets make the composite aerogels maintain their original highly porous structure after coating controlled PPy loading (Fig. S2). By adjusting the depositing time, we can obtain different PPy loaded composite electrodes (Fig. S4). We find that when the GO-GNR aerogels were loaded with 37.2 wt% PPy, the specific capacitance reaches a maximum value of 537 F g^{-1} at the scan rate of 2 mV s^{-1}, which is almost two-fold that of the aerogels without PPy (Fig. 5e, f). Even at a fast scan rate of 100 mV s^{-1}, it can still maintain a high specific capacitance of 218 F g^{-1} (Fig. S4), these results demonstrate that our GO-GNR aerogel can be an excellent material for supercapacitor.

Conclusions

In summary, we have fabricated multifunctional hybrid aerogels by introducing GNRs into GO sheets. The unique GO-GNR hybrid pore wall structure makes the aerogels highly porous, ultra-low density and compressible. The synergistic effect of the nanoribbons and graphene sheets makes the hybrid aerogels elastic after compression and our GO-GNR aerogels can recover with small residual strain (<3%) at the strain of ε = 80%. Owing to the large pore-size, robust and stable structure, our aerogels show high adsorption capacity to organic solvents and oils (100 to 350 times of aerogel weight), and a specific capacitance of 256 F g^{-1} for pristine arogels and 537 F g^{-1} for pseudo-polymer loaded aerogels. Our multifunctional hybrid aerogels may find potential applications in many fields such as environmental cleanup, and flexible electrodes for energy storage systems.

Acknowledgements

Y. Li and X. He acknowledge the Natural Science Foundation in China (NSFC 11272109) and the Ph. D. Programs Foundation of Ministry of Education of China

(20122302110065). A. Cao acknowledges NSFC (91127004, 51325202) and the Ph. D. Programs Foundation of Ministry of Education of China (20120001110076).

† Electronic Supplementary Information (ESI) available: [TEM of GNR-coated graphene sheet, SEM of PPy coated aerogels, FT-IR, XPS, XRD spectra of corresponding materials. CVs and calculated specific capacitances of the different PPy loaded GO-GNR electrode. Supercapacitive performance of typical graphene based aerogel]. See DOI: 10.1039/b000000x/

Notes and references

1 Geim, A. K.; Novoselov, K. S. The Rise of Graphene. *Nat. Mater.* 2007, **6,** 183-191.

2 Novoselov, K. S.; Fal'ko, V. I.; Colombo, L.; Gellert, P. R.; Schwab, M. G.; Kim, K. A Roadmap for Graphene. *Nature* 2012, **9,** 192-200.

3 Hummers, Wm. S., Jr.; Offeman, R. E. Preparation of Graphitic Oxide. *J. Am. Chem. Soc.* 1958, **80,** 1339.

4 Xu, Y. X.; Sheng, K. X.; Li, C.; Shi, G. Q. Self-assembled Graphene Hydrogel Via A One-step Hydrothermal Process. *ACS Nano* 2010, **4,** 4324-4330.

5 Wu, C.; Huang, X. Y.; Wang, G. L.; Lv, L. B.; Chen, G.; Li, G. Y.; Jiang, P. K. Highly Conductive Nanocomposites with Three-dimensional, Compactly Interconnected Graphene Networks Via A Self-assembly Process. *Adv. Mater.* 2013, **23,** 506-513.

6 Qiu, L.; Jeffery, Z. L.; Shery, L. Y. C.; Wu, Y. Z.; Li, D. Biomimetic Superelastic Graphene-Based Cellular Monoliths. *Nat. Commun.* 2012, **3,** 1241.

7 Lin, Y. R.; Gregory, J. E.; Colton, B.; Henry, A. S. Superhydrophobic Functionalized Graphene Aerogels. *ACS. Appl. Mater. Interfaces.* 2011, **3,** 2200-2203.

8 Zhang, X. T.; Sui, Z. Y.; Xu, B.; Yue, S. Y.; Luo, Y. J.; Zhan, W. C.; Liu, B. Mechanically Strong and Highly Conductive Graphene Aerogel and Its Use as Electrodes for Electrochemical Power Sources. *J. Mater. Chem.* 2011, **21,** 6494-6497.

9 Hu, H.; Zhao, Z. B.; Wan, W. B.; Yury, G.; Qiu, J. S. Ultralight and Highly Compressible Graphene Aerogels. *Adv. Mater.* 2013, **25,** 2219-2223.

10 Xu, Z.; Zhang, Y.; Li, P. G.; Gao, C. Strong, Conductive, Lightweight, Neat Graphene Aerogel Fibers with Aligned Pores. *ACS Nano* 2012, **6,** 7103-7113.

11 Zhao, J. P.; Ren, W. C.; Cheng, H. M. Graphene Sponge for Efficient and Repeatable Adsorption and Desorption of Water Contaminations. *J. Mater. Chem.,* 2012, **22,** 20197-20202.

12 Yao, H. B.; Ge, J.; Wang, C. F.; Wang, X.; Hu, W.; Zheng, Z. J.; Ni, Y.; Yu, S. H. A Flexible and Highly Pressure-Sensitive Graphene-Polyurethane Sponge Based on Fractured Microstructure Design. *Adv. Mater.* 2013, **25,** 6692-6698.

13 Xu, Y.; Lin, Z. Y.; Huang, X. Q.; Wang, Y.; Huang, Y.; Duan, X. F. Functionalized Graphene Hydrogel-Based High-Performance Supercapacitors. *Adv. Mater.* 2013, **25,** 5779-5784.

14 Wu, Z. S.; Yang, S. B.; Sun, Y.; Khaled, P.; Feng, X. L.; Mullen, K. 3D Nitrogen-Doped Grahene Aerogel-Supported Fe3O4 Nanoparticles as Efficient Electrocatalysts for the Oxygen Reduction Reaction. *J. Am. Chem. Soc.* 2012, **134,** 9082-9085.

15 Ren, W. C.; Cheng, H. M. When Two is Better Than One. *Nature* 2013, **497,** 448-4.

16 Sun, H. Y.; Xu, Z.; Gao, C. Multifunctional, Ultra-Flyweight, Synergistically Assembled Carbon Aerogels. *Adv. Mater,* 2013, **25,** 2554-2560.

17 Zhang, L.; Zhang, F.; Yang, X.; Long, G. K.; Wu, Y. P.; Zhang, T. F.; Leng, K.; Huang, Y.; Ma, Y. F.; Yu, A.; Chen, Y. S. Porous 3D Graphene-Based Bulk Materials with Exceptional High Surface Area and Excellent Conductivity for Supercapacitors. *Scientific Reports.* 2013, **3,** 1408.

18 Yan, Z.; Ma, L. L.; Zhu, Y.; Lahiri, I.; Hahm, M. G.; Liu, Z.; Yang, S. B.; Xiang, C. S.; Lu, W.; Peng, Z. W.; Sun, Z. Z.; Kittrell, C.; Lou, J.; Choi, W. B.; Ajayan, P. M.; Tour, J. M. Three-Dimensional Metal-Graphene-Nanotube Multifunctional Hybrid Materials. *ACS Nano* 2013, **7,** 58-64.

19 Zhi, J.; Zhao, W.; Liu, X. Y.; Chen, A. R.; Liu, Z. Q.; Huang, F. Q. Highly Conductive Ordered Mesoporous Carbon Based Electrodes Decorated by 3D Graphene and 1D Silver Nanowire for Flexible Supercapacitor. *Adv. Funct. Mater.* 2013, **24,** 2013-2019.

20 Kim, K. H.; Oh, Y. S.; Islam, M. F. Graphene Coating Makes Carbon Nanotube Aerogels Superelastic and Resistant to Fatigue. *Nat.Nanotechnol.* 2012, **7,** 562-566.

21 Peng, Q. Y.; Li, Y. B.; He, X. D.; Gui, X. C.; Shang, Y. Y.; Wang, C. H.; Wang, C.; Zhao, W. Q.; Du, S. Y.; Shi, E. Z.; Li, P. X.; Wu, D. H.; Cao. A. Y. Graphene Nanoribbon Aerogels Unzipped from Carbon Nanotube Sponges. *Adv. Mater.* 2014, DOI: 10.1002/adma.201305274.

22 Kosynkin, D. V.; Higginbotham, A. L.; Sinitskii, A.; Lomeda, J. R.; Dimiev, A.; Price, B. K.; Tour, J. M. Longitudinal Unzipping of Carbon Nanotubes to Form Graphene Nanoribbons. *Nature* 2009, **458,** 872-877.

23 Son, Y. W.; Marvin, L. C.; Steven, G. L. Energy Gaps in Graphene Nanoribbons. *Phy. Rev. Lett.* 2006, **97,** 216803.

24 Melinda, Y. H.; Barbaros, O.; Zhang, Y. B.; Philip, Kim. Energy Band-Gap Engineering of Graphene Nanoribbons. *Phy. Rev. Lett.* 2007, **98,** 206805.

25 Rafiee, M. A.; Lu, W.; Thomas, A. V.; Zandiatashbar, A.; Rafiee, J.; Tour, J. M.; Koratkar, N. A. Graphene Nanoribbon Composites. *ACS Nano* 2010, **4,** 7415-7420.

26 Yang, Z. B.; Liu, M. K.; Zhang, C.; Tjiu, W. W.; Liu, T. X.; Peng, H. S. Carbon Nanotubes Bridged with Graphene Nanoribbons and Their Use in High-Efficiency Dye-Sensitized Solar Cells. *Angew. Chem. Int. Ed.* 2013, **52,** 3996-3999.

27 Li, L.; Addul-Rahman, O. R.; James, M. T. Graphene-Wrapped MnO2-Graphene Nanoribbons as Anode Materials for High-Performance Lithium Ion Batteries. *Adv. Mater.* 2013, **25,** 6298-6302.

28 Bai, J. W.; Duan, X. F.; Huang, Y. Rational Fabrication of Graphene Nanoribbons Using a Nanowire Etch Mask. *Nano lett.,* 2009, **9,** 2083-2087.

29 Jiao, L. Y.; Zhang, L.; Wang, X. R.; Diankov, G.; Dai, H. J. Narrow Graphene Nanoribbons from Carbon Nanotubes. *Nature* 2009, **458,** 877-880.

30 Ma, L.; Wang, J. L. Ding, F. Recent Progress and Challenges in Graphene Nanoribbon Synthesis. *ChemPhysChem* 2013, **14,** 47-54.

31 Tour, J. M.; James, D. K. The Chemical Synthesis of Graphene Nanoribbons-A Tutorial Review. *Macromol. Chem. Phys*. 2012, **213,** 1033-1050.

32 Marcano, D. C.; Kosynkin, D. V.; Berlin, J. M.; Sinitskii, A.; Sun, Z. Z.; Slesarev, A.; Alemany, L. B.; Lu, W.; Tour, J. M. Improved Synthesis of Graphene Oxide. *ACS Nano* 2010, **4,** 4806-4814.

33 Wei, G.; Miao, Y. E.; Zhang, C.; Yang, Z.; Liu, Z. Y.; Tjiu, W. W.; Liu, T. X. Ni-Doped Graphene/Carbon Cryogels and Their Applications as Versatile Sorbents for Water Purification. *ACS Appl. Mater. Interfaces* 2013, **5,** 7584-7591.

34 Liu, Y.; Ma, J. K.; Wu, T.; Wang, X. R.; Huang, G. B.; Liu, Y.; Qiu, H. X.; Li, Y.; Wang, W.; Gao, J. P. Cost-Effective Reduced Graphene Oxide-Coated Polyurethane Sponge as A Highly Efficient and Reusable Oil-Absorbent. *ACS Appl. Mater. Interfaces* 2013, **5,** 10018-10026.

Table of Contents

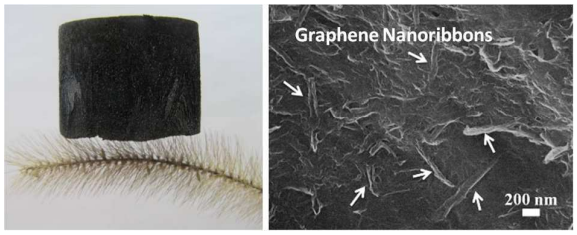

Highly porous and elastic aerogels consisting of graphene sheets and nanoribbons can be used as adsorbents and supercapacitor electrodes